A new perspective on the $\delta^{13}C$ signal preserved in speleothems using LC-IRMS analysis of bulk organic matter and compound specific stable isotope analysis.

Alison J Blyth[1*], Colin I. Smith[2], Russell N. Drysdale[3,4]

[1]WA-OIGC, Department of Chemistry, Chemistry and Resources Precinct, Curtin University, GPO Box U1987, Perth, WA 6845, Australia.

[2]Department of Archaeology, Environment and Community Planning, La Trobe University Melbourne, Victoria, 3086, Australia.

[3]Dept of Resource Management and Geography, Melbourne School of Land and Environment, University of Melbourne, Victoria 3010, Australia

[4]EDYTEM, UMR CNRS 5204, Université de Savoie, 73376 Le Bourget du Lac cedex, France

*Corresponding author. Current address: WA-OIGC, Chemistry and Resources Precinct, Curtin University, GPO Box U1987, Perth, WA 6845, Australia
Email: Alison.Blyth@curtin.edu.au
Phone: +61 8 9266 9388, Fax: +61 8 9266 2300

Abstract

The analysis of $\delta^{13}C$ in speleothem calcite is established as a palaeoenvironmental proxy, but records can often be complex to interpret due to multiple controls on the signal. Here we present a novel palaeoenvironmental application of non-purgeable organic carbon (NPOC) $\delta^{13}C$ analysis and compound-specific isotope analysis (CSIA) to speleothems, and compare the resultant signals to a conventional calcite $\delta^{13}C$ record. By accessing the carbon pool held in molecular organic matter, we are able for the first time to produce stable isotope records complementary to the CO_2-derived signal from the speleothem calcite, and begin to identify separate ecological and climatic controls. In this sample from north-west Scotland, the calcite $\delta^{13}C$ record and the NPOC $\delta^{13}C$ both show fluctuations at a period of increasing wetness and change from birch woodland to more open peatland, the NPOC signal having a strong correlation with biomarkers for vegetation change. We interpret an inverse correlation between the NPOC and CO_2 $\delta^{13}C$ signals as primarily driven by changes in soil conditions impacting upon microbial activity, with decreased activity leading to a reduction in ^{13}C enrichment of the residual organic matter (the NPOC fraction), and an increase in $\delta^{13}C$ in the CO_2 pool (calcite) due to a decrease in respired ^{12}C. This opens the way for the application of parallel analyses to distinguish between soil conditions and vegetation parameters as the primary control on a record, and highlights the advantage of combining both inorganic and organic geochemical techniques in the palaeoenvironmental interpretation of stable carbon isotopic records.

Keywords

Speleothem; organic carbon; $\delta^{13}C$; LC-IRMS; vegetation; soil

1. Introduction

The analysis of stable isotopes in speleothem calcite is a well-established technique in Quaternary research, with oxygen isotopes ($\delta^{18}O$) particularly widely used to investigate past climate systems (for reviews see McDermott, 2004; Lachniet, 2009). However, carbon stable isotopes ($\delta^{13}C$) are also of interest (e.g. Dorale et al., 1992; Genty et al. 2003, 2006), but are less well understood due to the complexity of the controls on the system. In an ideal closed system, speleothem carbon will be sourced 50% from the dissolved bedrock, and 50% from soil CO_2. However, studies of ^{14}C in modern speleothem samples have indicated that the carbon in speleothem carbonate is actually predominantly sourced (80-90%) from soil CO_2 (Genty & Massault, 1999; Genty et al., 2001; Griffiths et al. 2012; Hua et al. 2012). The soil CO_2 signal is in turn influenced by atmospheric CO_2 composition, and processed via vegetation input and microbial respiration. Changes in the $\delta^{13}C$ of stalagmite calcite have frequently been interpreted as changes in the overlying vegetation regime between C3 and C4 plants (e.g. Dorale et al., 1998; Denniston et al., 2001). However, whilst this interpretation is highly appropriate for some sites, regions and timescales, significant fluctuations in $\delta^{13}C$ have also been observed at sites where there is no evidence for major changes in the ratio of C4 to C3 plants, and where the known climatic parameters make such changes unlikely (Baker et al., 1997; Hellstrom et al., 1998; Genty et al., 2003; 2006). Furthermore, a study of an Ethiopian stalagmite known to have grown during a switch in overlying vegetation from predominantly C3 arboreal scrub to predominantly C4 crops showed that, although the change in vegetation was detected in the stalagmite lipid record, it was not clearly marked in the calcite $\delta^{13}C$ signal, which was time lagged and smoothed (Blyth et al., 2007). Consequently, the other factors controlling carbon isotope values need equal consideration.

In the soil, beyond the initial vegetation input, the CO_2 signal will also be affected by the degree of microbial activity, the mixing of different organic-matter pools, temperature-dependent fractionation of the organic carbon used in microbial respiration, and the degradation state of the

63 organic matter involved (Benner et al., 1987; Andrews et al., 2000; Biasi et al., 2005), as well as the
64 residence time within the soil. Microbial activity is considered especially important, with microbes
65 preferentially using and therefore respiring ^{12}C. Genty et al. (2003, 2006) proposed that increased
66 microbial activity and increased vegetation cover result in a decrease in $\delta^{13}C$ in the soil CO_2 pool and,
67 consequently, in speleothems. Vegetation cover and microbial activity clearly link back to climate,
68 especially temperature and rainfall, potentially making $\delta^{13}C$ a sensitive climatic indicator.
69 Further modification of the $\delta^{13}C$ signal can occur during transport of carbon to the
70 stalagmite, as residence time of the water in the aquifer may also affect the isotopic composition as
71 varying degrees of further processing of organic matter and calcite precipitation occur en route to
72 the cave. These factors can also be largely controlled by climate, including changes in rainfall, and
73 climatically driven fluctuations in biogenic activity and turnover (Genty et al., 2003; 2006). For
74 example, where periods of low rainfall cause a reduction of aquifer recharge, and a resultant
75 dewatering of the fractures above a cavern, this can cause degassing of CO_2 from pore waters and
76 the precipitation of calcite along the surface of fractures, a process termed 'prior calcite
77 precipitation' (Fairchild et al. 2000). Although calcite precipitation causes preferential loss of ^{13}C
78 from the source waters to the solid phase, this is more than offset by preferential loss of ^{12}C from
79 the source waters through CO_2 degassing (Dulinski & Rosanski 1990). Thus, an interval of decreased
80 rainfall can result in higher speleothem $\delta^{13}C$ values. Lastly, even after transport to the cave, kinetic
81 fractionation during calcite precipitation due to rapid degassing of the drip water can also be an
82 issue (Fantidis & Enhalt, 1970; Hendy, 1971; Wiedner et al., 2008).
83 This wide range of potential controls and complicating factors can make it very difficult to
84 interpret changes in $\delta^{13}C$ in speleothem calcite in a palaeoenvironmental context. Some factors,
85 such as kinetic fractionation, affect more than one proxy and so can be tested by looking for
86 covarying chemical signals (e.g. the Hendy test, which looks at the variation in carbon and oxygen
87 isotopes along a lamina). However, other factors, especially those affecting the parent soil CO_2
88 signal, such as vegetation type or changes in microbial activity, are extremely difficult to disentangle,

89 especially where comparative proxies or contextual information about environmental change are
90 not present. Therefore, extending the types of $\delta^{13}C$ records we can recover, and particularly
91 increasing the detail at which we can investigate different carbon and organic matter pools, is
92 essential to gaining a better understanding of palaeoenvironmental signals in speleothems.
93 Traditional $\delta^{13}C$ analysis only accesses one carbon pool in speleothems – that released as
94 carbon dioxide on dissolution of the calcite with acid, i.e. that derived from CO_2 dissolved in the
95 drip-water. However, a second pool exists, consisting of carbon contained in organic molecules
96 entrapped within the calcite, which has not previously been the subject of isotopic analysis in
97 speleothems. It can be assumed to have two main sources: molecules derived from the soil and
98 molecules derived from *in situ* cave organisms (Blyth et al., 2008). The soil component will in turn
99 consist of plant material, microbial material, and degradation products. The isotopic composition of
100 this organic matter can be analysed in two ways: via analysis of the bulk organic matter, or via
101 compound specific isotope analysis (CSIA).
102 CSIA permits measurement of the isotopic composition of particular molecule groups. It is a
103 rapidly expanding technique, which is used in a wide range of research fields including
104 palaeoenvironmental research, forensics (e.g. Benson et al., 2006 and references therein), and
105 pollution chemistry (e.g. Thullner et al., 2012), amongst others. In the palaeoenvironmental context,
106 CSIA of $\delta^{13}C$ is generally used to assess the sources of organic matter within a record e.g. C3 vs. C4
107 plants; terrestrial vs. aquatic input (e.g. Talbot & Johannessen, 1992; Brincat et al., 2000; Volkman et
108 al., 2008), with increasing work focusing at a species-specific level (e.g. Jacob et al., 2008; Brader et
109 al., 2010). A major limitation in the application of CSIA to contexts such as stalagmites is the sample
110 sizes required, with the lower limit of detection requiring 5 ng of carbon per injection for each
111 compound of interest measured. For *n*-alkanes (which are saturated hydrocarbon chains) in the
112 range of C_{23} – C_{33}, carbon forms approximately 85% of the molecular weight. An absolute minimum
113 requirement of 5 ng of carbon therefore requires around 6 ng of compound. Data collected for
114 previous studies (Blyth et al., 2006; 2007; 2011) indicates that for the C_{31} *n*-alkane the abundance

ranges from 2 – 80 ng / g calcite. Taking into account the need to run multiple analyses per sample to recover reliable isotopic data, the potential for sample loss during initial extraction and clean-up, the need for prior GC-MS injection to check cleanliness of the sample, and the fact that working at the lowest limit of detection in itself increases the error of the technique, it is clear that not all stalagmite samples are likely to be amenable to the approach, and large, multi-gram calcite samples will be required. This may significantly reduce the viable temporal resolution of a time series.

Isotopic measurements on bulk organic matter preserved in speleothems offer the opportunity to gain an organic-derived signal at a much higher temporal resolution, as reliable measurements can be made via liquid chromatography – isotope-ratio mass spectrometry (LC-IRMS) on samples of as little as 100 mg of calcite (Blyth et al., 2013). This utilises LC-IRMS in flow-injection mode (i.e. without a chromatography column) to analyse non-purgeable organic carbon (NPOC, Albéric, 2011) in a liquid sample, and has the advantage that samples can be run directly from an acid digest without substantial wet-chemistry preparation. Bulk isotopic measurements have routinely been made on organic matter in other geochemical contexts, such as lakes, cave sediments, oceanic sediments, and peats and soils (e.g. Schelske & Hodell, 1995; Ménot & Burns 2001), but have not been widely made on speleothems due to the difficulty of removing the carbonate whilst neither contaminating nor biasing the remaining carbon isotope signal. The LC-IRMS technique resolves this problem, but is not without its own issues, in that what is measured is, in reality, not total NPOC, but the acid-soluble fraction, as acidic solutions will cause precipitation of some organic molecules, especially the humic acids. However, the existence of the technique nonetheless opens up a new field of study in stable carbon isotope records in stalagmites.

Here we present an integrated carbon isotope data set from a 2000-year-old stalagmite from Assynt in Scotland. The sample has previously been analysed for lipid biomarker content and has a known environmental and climatic history (Blyth et al., 2011). This makes it an ideal test sample for investigating the controls on and relationships between the various carbon isotope signals.

2. Methods and materials

2.1 Site and sample

The stalagmite sample, Tral-1, is a small (75 mm tip to base) strongly laminated specimen collected from Lower Traligill Cave in Assynt, north-west Scotland in 2003. It has previously been dated by U-Th disequilibrium dating (Blyth et al., 2011), with a basal age of 2200 years. The region has a mean annual air temperature of 7.2 °C and a maritime climate, with annual precipitation of >1900 mm (Baker et al., 1999). The area directly around the cave is overlain by thin mineral soils, supporting Calluna and grasses, while the valley upstream is primarily covered by peatland dominated by Calluna, Erica and Cyperaceae, with discontinuous areas of Sphagnum cover (Charman et al., 2001). Peat-core analysis indicates that this vegetation regime has persisted in the area for at least the last 3 ka, although prior to 1 ka, birch woodland was an additional major ecosystem component (Charman et al., 2001). It is believed that the land directly above the cave suffered slope collapse and soil / peat loss during the Little Ice Age around 300 years ago, which is reflected in the very top of the stalagmite as multiple hiatuses, and limited calcite deposition (Blyth et al., 2011).

2.2 Extraction method for NPOC and analysis by LC-IRMS

Samples for bulk NPOC $\delta^{13}C$ analysis were drilled manually with a fixed drill in a continuous series at intervals of 5 mm, providing samples of approximately 400 mg of calcite. Prior to drilling the surface of the stalagmite was rinsed with solvent cleaned 3M hydrochloric acid to remove external contamination.

Calcite powder samples of 100 – 200 mg were digested in 3 M phosphoric acid at a concentration of 1 ml acid / 100 mg powder. Phosphoric acid was used rather than hydrochloric

(which is conventionally used in stalagmite digestion, e.g. Blyth et al., 2006) because the halides in the hydrochloric acid were found to interfere with the action of the oxidant in the LC-MS run, resulting in unreliable isotopic data (Alberic 2011; Blyth et al., 2013). After complete digestion of the calcite, aliquots of samples were transferred to 1.8 ml autosampler vials and dissolved carbon dioxide was removed under vacuum in a rotary vacuum concentrator. Tests showed that vacuum treatment of one hour removed DIC to below the limit of detection, without affecting the organic isotope signal. After vacuum treatment, samples were sealed with caps, and transferred to the LC-IRMS instrument for analysis.

Stable-isotope analysis was carried out using a Thermo Scientific LC-IRMS (consisting of an Accela autosampler and Accela 600 pump attached to a Delta V plus isotope ratio mass spectrometer via an LC-Isolink). Reagents and mobile phase were made with MilliQ water, degassed under vacuum and sonication for 1 hour and afterwards constantly sparged with helium. The analytical method is described in Blyth et al. (2013). In brief, analysis was made in flow-injection mode using a mobile phase of dilute sulphuric acid pH 4.0-4.2 (100 µl of 1:50 H_2SO_4 in 1 L of MilliQ water) running at a flow rate of 300 µl min^{-1} maintained at 20 °C using the column oven. For each run 20 µl of sample was injected using the autosampler, and oxidation of the organic carbon was achieved using a catalyst of 1.28 M H_3PO_4 (flow rate 20 µl min^{-1}) and oxidant of 0.13 M $Na_2S_2O_8$ (flow rate 20 µl min^{-1}). The oxidation reactor in the LC-Isolink was maintained at 99.9 °C. Run time was 5 minutes with measurements made relative to the second of two 20 s reference-gas pulses at the start of the run; three more reference-gas pulses were used after the analyte peak had appeared to check for drift over the run. The reference gas is calibrated to a $\delta^{13}C$ value of -22.92‰ VPDB using USGS-41 Glutamic acid +37.626‰ VPDB as an international standard. As this is an enriched standard chosen due to necessity of availability, and not ideal for calibrating natural samples, a series of commercial amino acid standards (Sigma Aldrich) were also analysed. These in house standards had an isotopic range of -7.6‰ to -31.6‰, bracketing the reference gas and the expected stalagmite values, and had previously had their isotopic values confirmed on an elemental analyser

193 (Smith et al., 2009). These gave satisfactory results, confirming that the USGS-41 calibration is
194 robust. Between analytical runs phosphoric acid blanks were measured to help clean the sample
195 loop and reduce sample carry over, as well as prevent calcium phosphate build up in the in-line
196 filters. Needle flushing was performed with a non-degassed mobile phase solution. Previous
197 method development work (Blyth et al., 2013) has shown the LC-IRMS technique to have acceptable
198 precision of around +/- 0.2‰ across a linearity range of 1000 – 9000 mV, equating to an organic
199 carbon abundance of 4 – 23 µg per sample.
200
201 **2.3. $\delta^{13}C$ calcite**
202
203 Samples for $\delta^{13}C$ analysis of calcite were drilled in a continuous series using a micromilling
204 lathe employing the method described by Drysdale et al. (2007). The stalagmite section was first
205 routed to produce a ledge ~2.5 mm thick and ~3.5 mm deep. The ledge was sampled at consecutive
206 100 µm increments using a milling bit. Due to the highly visible, parallel-tabular banding pattern of
207 the stalagmite, sampling uncertainty is unlikely to exceed ± 100 µm from the nominal centre point of
208 each sampling increment.
209 The stable isotopic composition of the calcite powders was determined on ~0.8 mg samples
210 using a GV Instruments GV2003 continuous-flow isotope-ratio mass spectrometer at the University
211 of Newcastle, Australia. Powders were acidified at 70 °C using 105% phosphoric acid and isotope
212 measurements made on the CO_2 evolved from the reaction. Sample results were converted to the
213 conventional 'delta' notation on the Vienna Pee Dee Belemnite scale using an internal standard of
214 Carrara Marble (NEW-1) previously calibrated to NBS-19.
215
216 **2.4 Compound specific isotope analysis**
217

Compound-specific isotope analysis was carried out on the previously analysed lipid samples reported in Blyth et al. (2011). To recover clean *n*-alkane fractions, the total lipid extract was placed on a silica gel column and the non-polar fraction recovered by elution with hexane. Samples suspended in hexane were manually injected into a Finnigan Trace GC, coupled to a Thermo Finnigan MAT 253 isotope-ratio mass spectrometer at The Open University, UK. GC oven temperature was held for 1 min at 50 °C and then programmed at 5 °C min^{-1} to 310 °C, the final temperature was held for 9 min. The isotopes were measured relative to a NIST standard. C_{25}, C_{27}, C_{29}, and C_{31} *n*-alkanes were measured. Analytical variability established via repeat injections of a C_{19} *n*-alkane standard.

3. Results and discussion

3.1 Results

The $\delta^{13}C$ results from the NPOC preserved in Tral-1 show an acceptable precision with eleven of the 15 samples having an SD across three analyses of 0.1 – 0.4‰ (Fig. 1.). The remaining four samples have SDs of 0.7, 0.7, 0.8, and 1‰. These levels of precision are not ideal, but are acceptable in low abundance samples. Peak amplitudes for m/z 44 in Tral-1 were around 1000 mV. The overall isotopic range in the sequence is 6.4‰ (-20.1 to -26.5‰).

The $\delta^{13}C$ analyses of the stalagmite calcite show an overall isotopic range of 4.5‰ (-8 to -12.5‰). The analytical precision of the technique was 0.05‰.

For the compound specific isotope analyses, the errors were harder to establish, as subsamples from the main body of the stalagmite were found to contain alkane abundances near the measurement limits for the technique, which meant each sample could only be injected once, without repeats. The analytical precision was established by repeat injection of a C_{19} *n*-alkane standard, which gave a repeatability of 0.15‰. An approximated error for the samples was provided by running five analytical repeats on the subsample from the top few mm of the stalagmite, which

was much richer in organics than the other samples. This gave a range of standard deviations across the four compounds of interest of 0.2 – 0.6‰. In the time-series the compound-specific carbon isotopes vary from -29.8‰ to -34.4‰, which is within the expected range for *n*-alkanes derived from C3 vegetation (Rieley et al., 1991; Collister et al., 1994; Bi et al., 2005). There is systematic depletion of isotopic values with increasing carbon chain length, a characteristic that has been widely noted in *n*-alkanes from other environmental contexts, and relates to isotopic fractionation in the plant tissue during compound synthesis (e.g. Rieley et al., 1991; Spooner et al., 1994; Brincat et al., 2000). Within each carbon chain, the time-series range is 2.5‰ for $C_{25, 27, 29}$ and 1.8‰ for C_{31}. This is a noticeably smaller variation than that seen in either the NPOC or calcite. Figure 2 shows the CSIA data for the sample, and it can be seen that the signals for the four compounds only partially covary. When linear regression is performed, it is found that C_{25} (the dominant lipid peak in most of the sub-samples) stands out, with no real correlation with C_{27} and C_{29} (r^2 = 0.22, and 0.11 respectively), and a moderate correlation with C_{31} (r_2 = 0.58). C_{27} and C_{29} superficially correlate strongly together (r^2 = 0.73), but this is actually driven by a single data point. The differences may be due to natural environmental differences in the source of the different compounds; in vegetation terms, in temperate environments, C_{25} is a known major component of peat derived signals, while C_{31} is more commonly associated with grasses, and C_{27} and C_{29} with trees, although microbial processing can interfere with this simple association, especially at lower chain lengths (Rieley et al., 1991b; Marseille et al., 1999; Pancost et al., 2002; Blyth et al., 2007). Alternatively, there may be analytical artefacts present, resulting from the low sample size and lack of repeat injections. Therefore, whilst we consider the CSIA signal interesting, and worthy of further investigation in speleothems either richer in organics or able to provide larger calcite samples, at this stage, we feel it should not be over-interpreted.

3.2 Changes through time

Figure 3 shows the variation in three isotopic signals along the length of the stalagmite (calcite, NPOC and C_{25} n-alkane), in addition to the results of the C_{27}/C_{31} *n*-alkane biomarker ratio (previously taken as a vegetation proxy in this stalagmite by Blyth et al. (2011)). The first point to note is that there is broad covariance in all the signals in terms of when changes occur, with all the signals showing a change around 1000 years ago. However, the magnitude and direction of the change varies between the records. In particular, the NPOC and calcite records are inversely correlated, with the NPOC record decreasing (becoming more negative, or less enriched with ^{13}C) after 1000 years, while the calcite record increases (becomes more positive, or relatively more enriched with ^{13}C). The magnitude of change is also much greater and more marked in the NPOC record. To investigate the strength of these apparent relationships, we carried out linear regression between the signal curves for the calcite, NPOC, and vegetation biomarker signals. The CSIA signal was excluded due to the concerns about reliability outlined in section 3.1. We also excluded points from the top of the stalagmite, above the major hiatus at approximately 300 years (area represented by a grey box on Fig. 3). This is because the calcite in this portion contains multiple hiatuses and associated crusts, as well as detrital flood events, and therefore it is not directly comparable in formation, organic content or fabric to the bulk of the stalagmite, which has formed without any discernible hiatuses via normal drip deposition. Fig. 4 shows the results of the linear regression. The NPOC and calcite isotopic signals show a moderate inverse correlation ($r^2 = 0.57$, $p < 0.005$), while the NPOC signal and calcite signals show clear relationships with the C_{27}/C_{31} *n*-alkane ratio ($r^2 = 0.73$, $p < 0.05$; $r^2 = 0.70$, $p < 0.05$).

Previous palaeoenvironmental interpretations of data from this stalagmite have noted that at around 1000 years ago there was a decrease of birch woodland in the area, as demonstrated by two independent records – peat-core data (Charman et al., 2001) and the lipid biomarker record in this stalagmite (Blyth et al., 2011). In the latter case there is a marked change in the C_{27}/C_{31} *n*-alkane record in favour of C_{31}, indicating a decrease in tree cover in favour of herbaceous vegetation. The synchronisation of the changes in the isotope records reported here (at around 1000

296 years ago) with each other and the previous lipid biomarker records indicates that the isotope
297 signals are recording genuine environmental responses. The time interval following this change and
298 covered by the more negative isotopic signal in the NPOC record (around 1000 – 300 years ago) also
299 includes the periods of highest rainfall for the area during the last 2 ka (Proctor et al., 2000, 2002;
300 Trouet et al., 2009), which are characterised in the broader lipid record by a substantial increase in
301 soil and plant derived organic matter (Blyth et al., 2011). This was hypothesised to be the result of
302 increased throughput of soil organic matter due to increased drip flow to the stalagmite, an
303 argument supported by a decreased calcite growth rate (due to decreased soil respiration of CO_2
304 resulting from soil water saturation).
305 If the changes in the isotopic records were being driven by the vegetation change alone, we
306 might expect both CO_2 and NPOC records to move in the same direction, becoming more or less
307 enriched in response to isotopic changes in the plants, which are transmitted by root respiration and
308 plant material input. However, in reality, we see an inverse relationship between the calcite $\delta^{13}C$
309 and the NPOC signal, which we suggest is dominantly driven by changes in the soil conditions,
310 occurring in parallel to, but not necessarily controlled by, the vegetation change. The calcite signal is
311 recording the dissolved CO_2, which is predominantly controlled by soil respiration, consisting of a
312 vegetation signal, significantly modified by microbial activity. It is known that soil microbes
313 selectively use and therefore respire ^{12}C, meaning that at times of increased microbial activity the
314 CO_2 pool will be relatively depleted in $\delta^{13}C$ (due to the increased ^{12}C input), and in times of
315 decreased activity, it will be relatively ^{13}C enriched (due to the reduction in respired ^{12}C).
316 Conversely, increased microbial activity leads to the ^{13}C enrichment of residual organic matter (such
317 as that contained in the NPOC fraction) due to the preferential use of ^{12}C, and decreased microbial
318 activity will lead to a more negative $\delta^{13}C$, due to the cessation of this enrichment. Thus, it is clear
319 that when soil microbial activity changes significantly and forms the dominant control on the
320 isotopic signal, we would expect the CO_2 and NPOC pools to react in opposite directions. In Tral-1
321 we see the inverse movement of the two signals commencing with a period of increased soil

wetness and increased peat formation, which by restricting oxygen in the soil is likely to have led to a decrease in microbial activity.

3.3. Implications for the use of speleothem $\delta^{13}C$ in palaeoenvironmental research

We suggest that the use of parallel calcite CO_2 and NPOC analyses has significant potential utility in improving our understanding of the controls on speleothem $\delta^{13}C$ signals, with an inverse signal correlation being a potential proxy for soil microbial activity as the dominant control. However, a number of issues remain requiring future investigation. Firstly, although one mechanism may form the predominant control on the isotopic record, it is highly unlikely that there will ever be only one single influence on the signal. For example, in the case of Tral-1, there is clearly a vegetation change occurring at the same time, and whilst the inverse relationship of the signals suggests this is not dominating the record, it will have an effect. We suggest that, analytical issues permitting, the best approach to establishing the extent of the vegetation-derived isotopic change is to interrogate the CSIA signal for selected plant-derived compounds. It has been noted that, in the case of Tral-1, the magnitude of isotopic change within each of the measured *n*-alkanes is smaller than that seen in either the CO_2 or NPOC records. This indicates that the isotopic change within the vegetation is modest, presumably because it is a change within different types of C3 vegetation, and not a significant contributor to the isotopic changes in the soil.

More complex to distinguish is the degree of microbial activity at the time of formation vs. the age of the carbon pools being transmitted to the speleothem, as a longer time exposed to moderate microbial activity might be expected to have the same effect on both $\delta^{13}C$ signals as a shorter time exposed to a more intense activity. In Tral-1, we know from lipid and stalagmite growth evidence that the increase in surface wetness was accompanied by an increase in drip-flow to the stalagmite and in fresh organic matter input. Therefore, it seems possible that there are two mechanisms (decreased microbial activity in the soil, and decreased exposure to microbial activity

348 due to faster through-flow) acting to move the microbial modification of the isotopic signal in the
349 same direction. The change in the type of organic matter input towards fresher (i.e. less ^{13}C
350 enriched) material may explain why the magnitude of the isotopic change is greater in the NPOC
351 signal compared to the CO_2 signal.

352 Another issue is using the isotopic signal and the hypothesised control to identify climatic
353 changes. Reduction of microbial activity in the soil may occur as a result of various climatic
354 parameters, including decreased temperature, increased soil moisture leading to soil saturation, or
355 conversely, excessive soil dryness. Extremes of climate can be ruled out by stalagmite growth, as
356 excessively dry or cold weather will retard stalagmite formation by preventing sufficient water flow,
357 but more moderate changes may lead to similar results. In the case of Tral-1, we can clearly identify
358 the climatic mechanism by combining the carbon isotope data with other records, and we suggest
359 that this is where a multi-proxy approach to extrapolating climatic records from stalagmites is the
360 optimal approach, using each signal to mutually inform the interpretation of the others, and so
361 provide the most in-depth environmental picture possible.

362

363 **4. Conclusion**

364

365 This study clearly shows that multiple stable carbon isotope records are preserved in
366 speleothems, and reflect different aspects of the soil carbon pools. This is the first time-series
367 application of NPOC isotopic measurements and CSIA in speleothems, and demonstrates that
368 useable, environmentally coherent signals can be recovered. CSIA in speleothems shows future
369 potential, with the C_{25} *n*-alkane record here showing a modest response to known climate and
370 vegetation change; however, issues around sample size and analytical repeatability need to be
371 resolved before the approach can be considered robust. Isotopic analysis of the NPOC appears a
372 highly successful technique, accessing a complementary data set to traditional calcite stable isotope
373 analysis, and significantly expanding the information we can recover from speleothem stable

isotopes, with the inverse correlation between the two records being a potential marker for microbial control of the signal. The research area would now benefit from further work investigating in more detail the link between the NPOC isotopic signal and the precise types of organic matter present, and the combined response of the $\delta^{13}C$ signals to environmental controls in other climatic and ecological contexts. Nonetheless, this integrated study clearly demonstrates the advantages of combining organic and inorganic geochemistry when interpreting climate records in general, and carbon isotopes in particular, in speleothems.

Acknowledgements

Funding for the study is gratefully acknowledged from AINSE (Research Fellowship to AJB), ARC (Future Fellowship to CS, grant number: FT0992258), and The Leverhulme Trust (Early Career Fellowship to AJB). Calcite micromilling and isotopic analyses were undertaken at the University of Newcastle, Australia. Compound specific isotope analyses were undertaken at The Open University, UK, and Dr Mabs Gilmour is thanked for her assistance with these. Dr Matthew Box assisted in sample drilling.

References:

Albéric, P. 2011. Liquid chromatography / mass spectrometry stable isotope analysis of dissolved organic carbon in stream and soil waters. Rapid Communications in Mass Spectrometry 25, 3012-3018.

Andrews, J.A., Matamala, R., Westover, K.M., Schlesinger, W.H. 2000. Temperature effect on the diversity of soil heterotrophs and the $\delta^{13}C$ of soil-respired CO_2. Soil Biology & Biochemistry 32, 699-706.

399 Baker, A., Ito, E., Smart, P.L., McEwan, R.F., 1997. Elevated and variable values of ^{13}C in speleothems
400 in a British cave system. Chemical Geology 136, 263-270.
401 Baker, A., Caseldine, C.J., Gilmour, M.A., Charman, D., Proctor, C.J., Hawkesworth, C.J., Phillips, N.,
402 1999. Stalagmite luminescence and peat humification records of palaeomoisture for the last 2500
403 years. Earth & Planetary Science Letters 165, 157-162.
404 Benner, R., Fogel, M.F., Sprague, E.K., Hodson, R.E. 1987. Depletion of ^{13}C in lignin and its
405 implications for stable carbon isotope studies. Nature 329, 708-710.
406 Benson, S., Lennard, C., Maynard, P., Roux, C. 2006. Forensic applications of isotope ratio mass
407 spectrometry – a review. Forensic Science International 157, 1-22.
408 Bi, X., Sheng, G., Liu, X., Li, C., Fu, J. 2005. Molecular and carbon and hydrogen isotopic composition
409 of *n*-alkanes in plant leaf waxes. Organic Geochemistry 36, 1405-1417.
410 Biasi, C., Rusalimova, O., Meyer, H., Kaiser, C., Wanek, W., Barsukov, P., Junger, H., Richter, A. 2005.
411 Temperature-dependent shift from labile to recalcitrant carbon sources of arctic heterotrophs.
412 Rapid Communications in Mass Spectrometry 19, 1401-1408.
413 Blyth, A.J., Farrimond, P., Jones, M. 2006. An optimised method for the extraction and analysis of
414 lipid biomarkers from stalagmites. Organic Geochemistry 37, 882-890.
415 Blyth, A.J., Asrat, A., Baker, A., Gulliver, P., Leng, M.J., & Genty, D. 2007. A new approach to
416 detecting vegetation and land-use change using high resolution lipid biomarker records in
417 stalagmites. Quaternary Research 68, 314-324.
418 Blyth, A.J., Baker, A., Colins, M.J., Penkman, KEH., Gilmour, M.A., Moss, J.S., Genty, D., Drysdale,
419 R.N., 2008. Molecular organic matter in speleothems as an environmental proxy. Quaternary Science
420 Reviews 27, 905-921.
421 Blyth, A.J., Baker, A., Thomas, L., van Calsteren, P. 2011. A 2000 year lipid biomarker record
422 preserved in a stalagmite from north-west Scotland. Journal of Quaternary Science 26, 326-334.
423 Blyth, A.J., Shutova, Y., Smith, C., 2013. $\delta^{13}C$ analysis of bulk organic matter in speleothems using
424 liquid chromatography – isotope ratio mass spectrometry. Organic Geochemistry 55, 22-25.

425 Brader, A.V., van Winden, J., Bohncke, S.J.P., Beets, C.J., Reichart, G-J., de Leeuw, J.W. 2010.
426 Fractionation of hydrogen, oxygen, and carbon isotopes in n-alkanes and cellulose of three
427 *Sphagnum* species. Organic Geochemistry 41, 1277-1284
428 Brandes, J.A. 2009. Rapid and precise δ13C measurement of dissolved inorganic carbon in natural
429 waters using liquid chromatography coupled to an isotope-ratio mass spectrometer. Limnology and
430 Oceanography: Methods 7, 730-739.
431 Brincat, D., Yamada, K., Ishiwatari, R., Uemura, H., Naraoka, H. 2000. Molecular-isotopic
432 stratigraphy of long-chain *n*-alkanes in Lake Baikal Holocene and glacial age sediments. Organic
433 Geochemistry 31, 287-294.
434 Charman, D.J., Caseldine, C., Baker, A., Gearey, B., Hatton, J., Proctor, C., 2001. Palaeohydrological
435 records from peat profiles and speleothems in Sunderland, Northwest Scotland. Quaternary
436 Research 55, 223-234.
437 Collister, J.W., Rieley, G., Stern, B., Eglinton, G., Fry, B. 1994. Compound-specific $\delta^{13}C$ analyses of
438 leaf lipids from plants with differing carbon dioxide mechanisms. Organic Geochemistry 21, 619-
439 627.
440 Denniston, R.F., Gonzalez, L.A., Asmerom, Y., Polyak, V., Ragan, M.K., Saltzman, M.R. 2001. A high-
441 resolution speloethem record of climatic variability at the Allerod-Younger Dryas transition in
442 Missouri, central United States. Palaeogeography Palaeoclimatology Palaeoecology 176, 147-155.
443 Dorale, J.A., González, L.A., Reagan, M.K., Pickett, D.A., Murrell, M.T., Baker, R.G. 1992. A high-
444 resolution record of Holocene climate change in speleothem calcite from Cold Water Cave,
445 northeast Iowa. Science 258, 1626-1630.
446 Dorale, J.A., Edwards, R.L., Ito, E., González, L.A. 1998. Climate and vegetation history of the
447 Midcontinent from 75 to 25 ka: a speleothem record from Crevice Cave, Missouri, USA. Science 282,
448 1871-1874.

449 Drysdale, R., Zanchetta, G., Hellstrom, J., Fallick, A., McDonald, J. & Cartwright, I. 2007. Stalagmite
450 evidence for the precise timing of North Atlantic cold events during the early last glacial. Geology 35,
451 77-80.
452 Dulinski, M., Rozanski, R., 1990. Formation of $^{13}C/^{12}C$ isotope ratios in speleothems: A semidynamic
453 model. Radiocarbon 32, 7–16.
454 Fairchild, I.J., Borsato, A., Tooth, A.F., Frisia, S., Hawkesworth, C.J., Huang, Y., McDermott, F., Spiro,
455 B. 2000. Controls on trace element (Sr-Mg) compositions of carbonate cave waters: implications for
456 speleothem climatic records. Chemical Geology 166, 255-269.
457 Fantidis, J., Enhalt, D. 1970. Variations of carbon and oxygen isotopic composition in stalagmites and
458 stalactites: evidence of non-equilibrium isotopic fractionation. Earth & Planetary Science Letters 10,
459 136-144.
460 Genty, D., Massault, M., 1999, Carbon transfer dynamics from bomb-^{14}C and $\delta^{13}C$ time series of a
461 laminated stalagmite from SW France - Modelling and comparison with other stalagmite records.
462 Geochimica et Cosmochimica Acta 63, 1537-1548.
463 Genty, D., Baker, A., Massault, M., Proctor, C., Gilmour, M., Pons-Branchu, E., Hamelin, B. 2001.
464 Dead carbon in stalagmites: carbonate bedrock palaeodissolution vs. ageing of soil organic matter.
465 Implications for ^{13}C variations in speleothems. Geochimica et Cosmochimica Acta 65, 3443-3457.
466 Genty, D., Blamart, D., Ouahdi, R., Gilmour, M., Baker, A., Jouzel, J., Van-Exter, S. 2003. Precise
467 dating of Dansgaard-Oeschger climate oscillations in western Europe from stalagmite data. Nature
468 421, 833-837.
469 Genty, D., Blamart, D., Ghaleb, B., Plagnes, V., Causse, Ch., Bakalowicz, M., Zouari, K., Chkir, N.,
470 Hellstrom, J., Wainer, K., Bourges, F. 2006. Timing and dynamics of the last deglaciation from
471 European and North African $\delta^{13}C$ stalagmite profiles – comparison with Chinese and South
472 Hemisphere stalagmites. Quaternary Science Reviews 25, 2118-2142.

473 Griffiths, M.L., Fohlmeister, J., Drysdale, R.N., Hua, Q., Johnson, K.R., Hellstrom, J.C., Gagan, M.K.,
474 Zhao, J-x., 2012. Hydrological control of the dead carbon fraction in a Holocene tropical speleothem.
475 Quaternary Geochronology in press. http://dx.doi.org/10.1016/j.quageo.2012.04.001
476 Hellstrom, J., McCulloch, M., Stone, J., 1998. A detailed 31,000 year record of climate and
477 vegetation change from the isotope geochemistry of two New Zealand speleothems. Quaternary
478 Research 50, 167-178.
479 Hendy, C.H., 1971. The isotopic geochemistry of speleothems I. The calculation of the effects of
480 different modes of formation on the isotopic composition of speleothems and their applicability as
481 palaeoclimatic indicators. Geochimica et Cosmochimica Acta 35, 801-824.
482 Hua, Q., McDonald, J., Redwood, D., Drysdale, R., Lee, S., Fallon, S., Hellstrom, J., 2012. Robust
483 chronological reconstruction for young speleothems using radiocarbon. Quaternary Geochronology
484 in press. http://dx.doi.org/10.1016/j.quageo.2012.04.017
485 Jacob, J., Disnar, J-R., Bardoux, G. 2008. Carbon isotope evidence for sedimentary miliacin as a
486 tracer of Panicum milaceum (broomcorn millet) in the sediments of Lake le Bourget (French Alps).
487 Organic Geochemistry 39, 1077-1080.
488 Lachniet, M.S., 2009. Climatic and environmental controls on speleothem oxygen isotope values.
489 Quaternary Science Reviews 28, 412-432.
490 Marseille, F., Disnar, J.R., Guillet, B., Noack, Y., 1999. n-Alkanes and free fatty acids in humus and A1
491 horizons of soils under beech, spruce and grass in the Massif-Central (Mont-Lozère), France.
492 European Journal of Soil Science 50, 433–441.
493 McDermott, F., 2004. Palaeo-climate reconstruction from stable isotope variations in speleothems:
494 a review. Quaternary Science Reviews 23, 901-918.
495 Ménot, G., Burns, S.J. 2001. Carbon isotopes in ombrogenic peat bog plants as climatic indicators:
496 calibration from an altitudinal transect in Switzerland. Organic Geochemistry 32, 233-245.

497 Pancost, R.D., Bass, M., van Geel, B., Sinninghe-Damsté, J.S., 2002. Biomarkers as proxies for plant
498 inputs to peats: An example from a subboreal ombrotrophic bog. Organic Geochemistry 33, 675–
499 690.
500 Proctor, C.J., Baker, A., Barnes, W.L., Gilmour, M.A., 2000. A thousand year speleothem proxy record
501 of North Atlantic climate. Climate Dynamics 16, 815-820.
502 Proctor, C.J., Baker, A., Barnes, W.L., 2002. A three thousand year record of North Atlantic climate.
503 Climate Dynamics 19, 449-454.
504 Rieley, G., Collier, R.J., Jones, D.M., Eglinton, G., Eakin, P.A., Fallick, A.K. 1991. Sources of
505 sedimentary lipids deduced from stable carbon isotope analyses of individual *n*-alkanes. Nature 352,
506 425-427.
507 Rieley, G., Collier, R.J., Jones, D.M., Eglinton, G., 1991b. The biogeochemistry of Ellesmere Lake,
508 U.K.–I: Source correlation of leaf wax inputs to the sedimentary lipid record. Organic Geochemistry
509 17, 901–912.
510 Schelske, C.L., Hodell, D.A. 1995. Using carbon isotopes of bulk sedimentary organic matter to
511 reconstruct the history of nutrient loading and eutrophication in Lake Erie. Limnology and
512 Oceanography 40, 918-929.
513 Smith, C.I., Fuller, B.T., Choy, K., Richards, M.P. 2009. A three phase liquid chromatographic method
514 for δ13C analysis of amino acids from biological protein hydrolysates using LC-IRMS. Analytical
515 Biochemistry 390, 165-172.
516 Spooner, N., Rieley, G., Collister, J.W., Lander, M., Cranwell, P.A., Maxwell, J.R. 1994. Stable carbon
517 isotopic correlation of individual biolipids in aquatic organisms and a lake bottom sediment. Organic
518 Geochemistry 21, 823-827.
519 Talbot, M.R., Johannessen, T., 1992. A high resolution palaeoclimatic record for the last 27,500 years
520 in tropical West Africa from the carbon and nitrogen isotopic composition of lacustrine organic
521 matter. Earth and Planetary Science Letters 110, 23-37.

522 Thullner, M., Centler, F., Richnow, H-H., Fischer, A. 2012. Quantification of organic pollutant
523 degradation in contaminated aquifers using compound specific stable isotope analysis – review of
524 recent developments. Organic Geochemistry 42, 1440-1460.
525 Trouet, V., Esper, J., Graham, N.E., Baker, A., Scourse, J.D., Frank, D.C., 2009. Persistent positive
526 North Atlantic Oscillation mode dominated the Medieval Climate Anomaly. Science 324, 78-80.
527 Volkman, J.K., Revill, A.T., Holdsworth, D.G., Fredericks, D. 2008. Organic matter sources in an
528 enclosed coastal inlet assessed using lipid biomarkers and stable isotopes. Organic Geochemistry 39,
529 689-710.
530 Wiedner, E., Scholz, D., Mangini, A., Polag, D., Mühlinghaus, C., Segl, M. 2008. Investigation of the
531 stable isotope fractionation in speleothems with laboratory experiments. Quaternary International
532 187, 15-24.
533

List of figures

Figure 1. δ13C data for the NPOC samples. Error bars are ±1 SD on 3 repeats.

Figure 2. Graph showing the change in the $\delta^{13}C$ composition of individual *n*-alkanes through the stalagmite.

Figure 3. Time-series graph showing the changes in the calcite, NPOC and C_{25} n-alkane $\delta^{13}C$ signals, and the C_{27}/C_{31} *n*-alkane biomarker ratio through time. Dates (yrs BP) and environmental interpretation are taken from Blyth et al. (2011). The grey area on the left is the area of the stalagmite above the major hiatus at approximately 300 yrs, where the calcite fabric is affected by multiple hiatuses, and detrital flood events.

Figure 4. Scatter plots showing the linear regressions for; a) the NPOC and calcite $\delta^{13}C$ signals; b) NPOC $\delta^{13}C$ against the C_{27}/C_{31} lipid biomarker ratio; c) calcite $\delta^{13}C$ against the C_{27}/C_{31} lipid biomarker ratio.

Figure 1

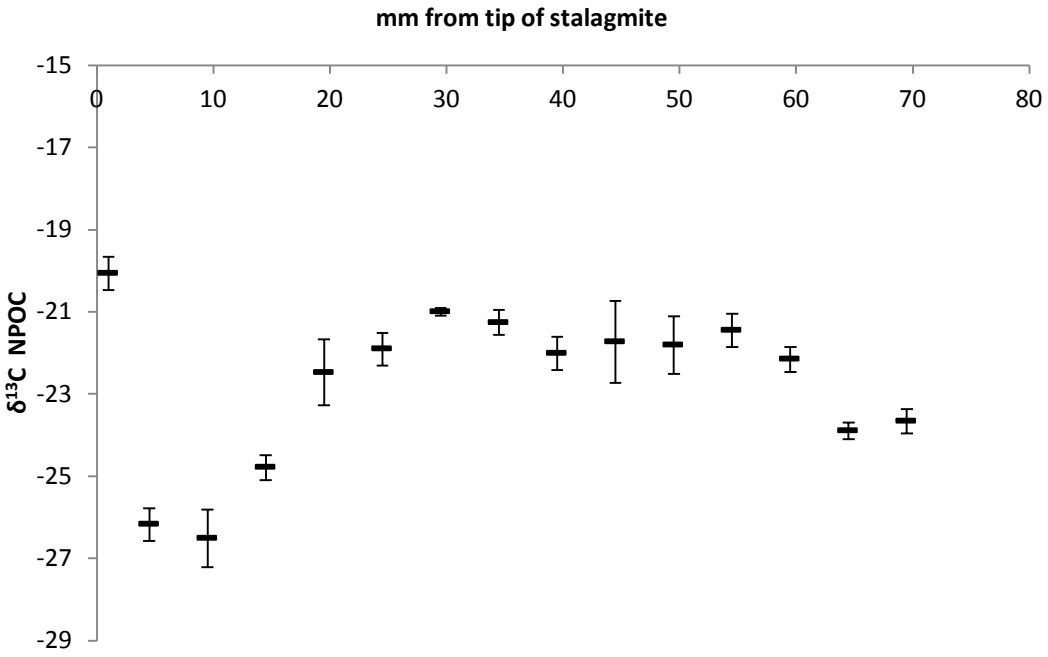
mm from tip of stalagmite
-15
-17
-19
-21
-23
-25
-27
-29
0
10
20
30
40
50
60
70
80
δ13C NPOC

Figure 2

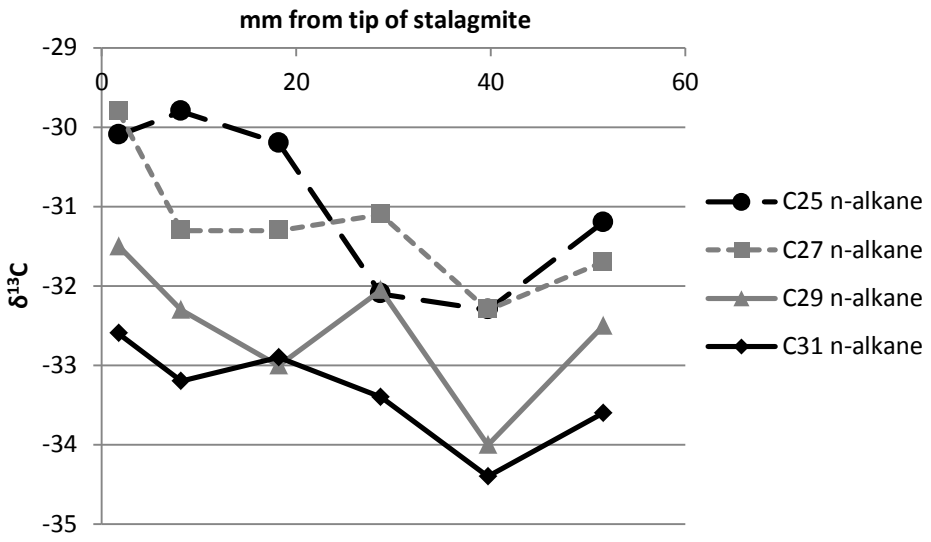
mm from tip of stalagmite
-29
-30
-31
-32
-33
-34
-35
0
20
40
60
δ13C
C25 n-alkane
C27 n-alkane
C29 n-alkane
C31 n-alkane

Figure 3

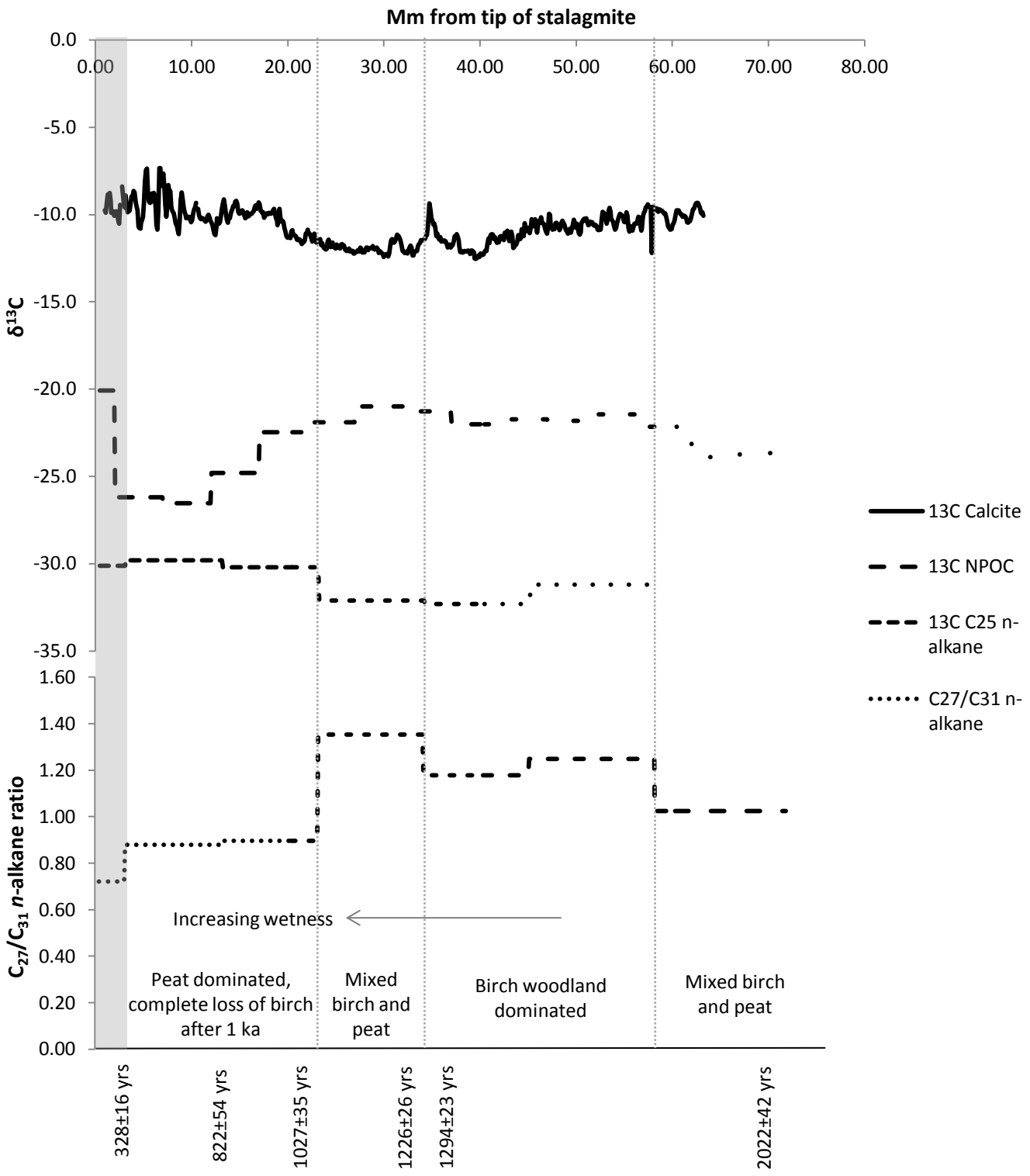
Mm from tip of stalagmite
0.0
0.00
10.00
20.00
30.00
40.00
50.00
60.00
70.00
80.00
-5.0
-10.0
-15.0
-20.0
-25.0
-30.0
-35.0
δ13C
1.60
1.40
1.20
1.00
0.80
0.60
0.40
0.20
0.00
C27/C31 n-alkane ratio
13C Calcite
13C NPOC
13C C25 n-alkane
C27/C31 n-alkane
Increasing wetness
Peat dominated, complete loss of birch after 1 ka
Mixed birch and peat
Birch woodland dominated
Mixed birch and peat
328±16 yrs
822±54 yrs
1027±35 yrs
1226±26 yrs
1294±23 yrs
2022±42 yrs

Figure 4

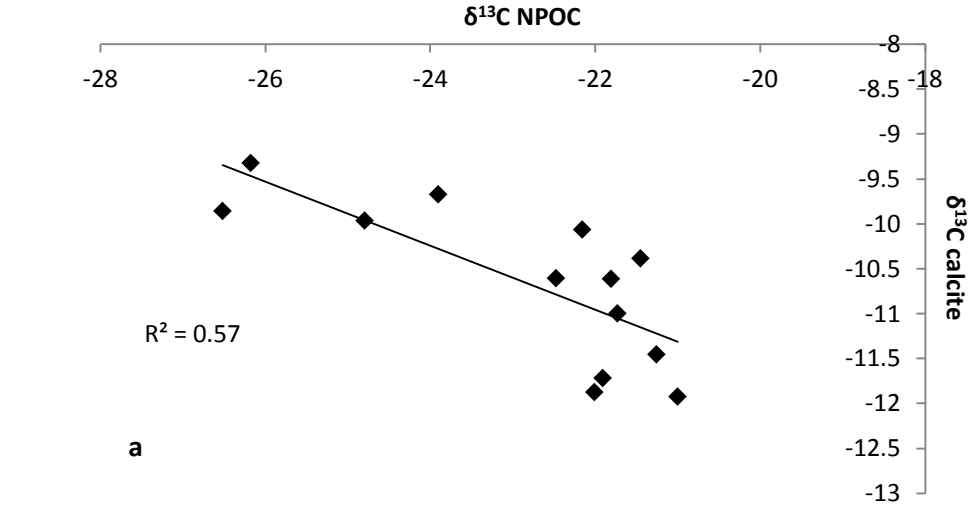
δ13C NPOC
-28
-26
-24
-22
-20
-18
-8
-8.5
-9
-9.5
-10
-10.5
-11
-11.5
-12
-12.5
-13
δ13C calcite
R² = 0.57
a

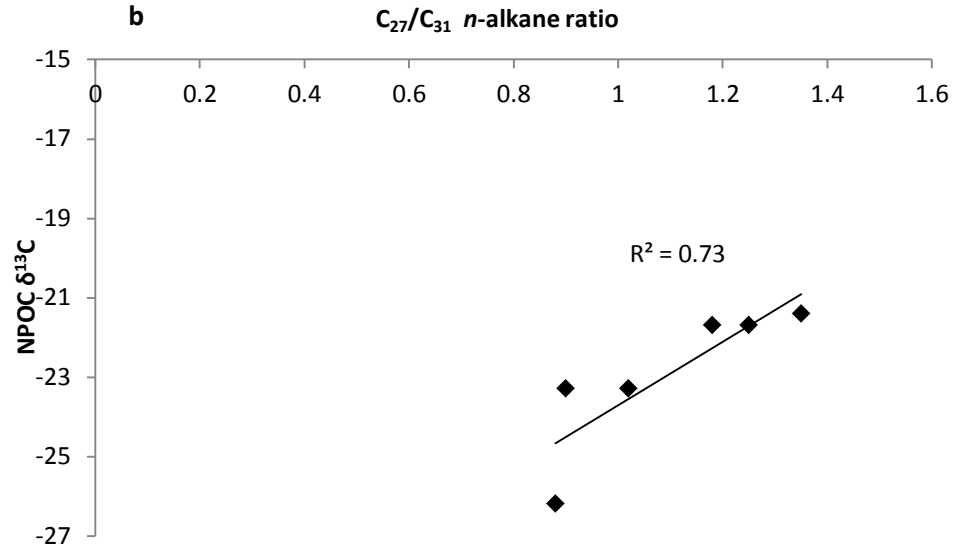
b
C27/C31 n-alkane ratio
-15
-17
-19
-21
-23
-25
-27
0
0.2
0.4
0.6
0.8
1
1.2
1.4
1.6
NPOC δ13C
R² = 0.73

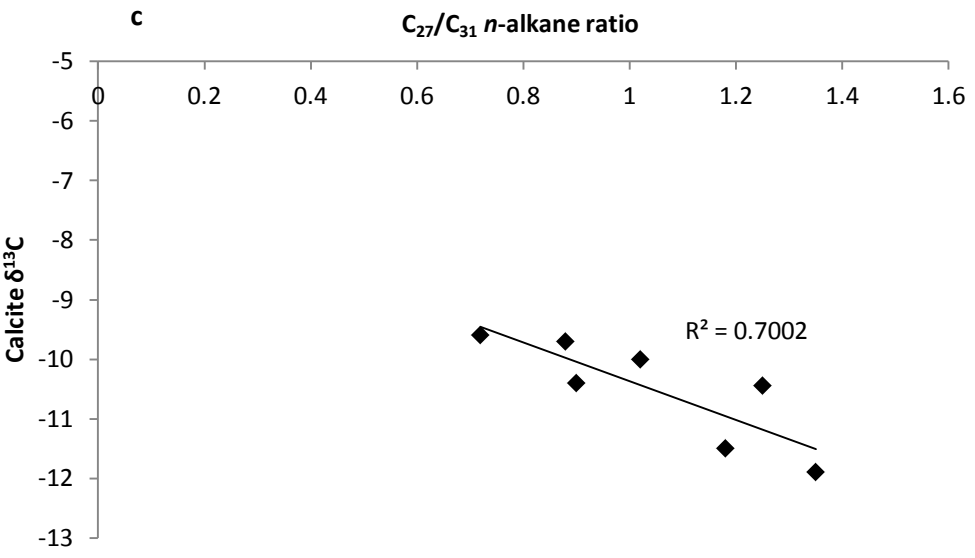
c
C27/C31 n-alkane ratio
-5
-6
-7
-8
-9
-10
-11
-12
-13
0
0.2
0.4
0.6
0.8
1
1.2
1.4
1.6
Calcite δ13C
R² = 0.7002